Am J Cancer Res 2020;10(11):3737-3751
www.ajcr.us /ISSN:2156-6976/ajcr0118615

Original Article

Circ-EEF2 facilitated autophagy via interaction with mir-6881-3p and ANXA2 in EOC

Min Yong[1], Jianguo Hu[1], Hongtao Zhu[1], Xinwei Jiang[1], Xiaolin Gan[1], Lina Hu[1,2]

[1]Department of Obstetrics and Gynecology, Second Affiliated Hospital, Chongqing Medical University, Linjiang Road, No. 76, Chongqing 400010, China; [2]Joint International Research Lab for Reproduction and Development, Ministry of Education, China

Received July 21, 2020; Accepted October 13, 2020; Epub November 1, 2020; Published November 15, 2020

Abstract: Circular RNAs, a special class of non-coding RNA with closed circular structure, have been increasingly proven to be involved in the progression of various tumors. However, the biological functions of circular RNAs in epithelial ovarian cancer (EOC) tissues remain a mystery. In this study, we detected the function of circEEF2 (has-circ-0048559) in EOC tissues. Firstly, the basic characteristics including closed circular structure and spliced mature sequence length of circEEF2 were confirmed. The location and expression in EOC tissues was detected by fluorescence in situ hybridization (FISH). The regulatory effect of circEEF2 on autophagy, proliferation, and invasion were investigated in SKOV3 and A2780 cells. The relationship between circEEF2 and mir-6881-3p was confirmed using dual-luciferase reporter gene assay. The binding of circEEF2 with ANXA2 was confirmed using RNA-pulldown assay and MALDI-TOF-MS. We found that the expression level of circEEF2 was higher in EOC tissue than in normal tissue. CircEEF2 promoted autophagy, proliferation, and invasion. CircEEF2-regulated EOC proliferation and invasion are closely related to the occurrence of autophagy. Mechanistically, circEEF2 harbor miR-6881-3p to upregulate the latter's targets ATG5 and ATG7. Moreover, circEEF2 could directly bind with ANXA2 to inhibit the expression of p-mTOR. In conclusion, findings of the current study illustrate that circEEF2 promoted autophagy, proliferation, and invasion of EOC by interacting with miR-6881-3p and ANXA2.

Keywords: circEEF2, autophagy, ANXA2, miR-6881-3P, epithelial ovarian cancer

Introduction

Epithelial ovarian cancer (EOC) is the most lethal malignant disease of female reproductive system [1]. In most patients, EOC is initially diagnosed at an advanced stage with evidence of abdominal dissemination of the disease. The standard therapeutic strategy involves surgical debulking combined with adjuvant chemotherapy [2]; however, at least 75% of patients will develop recurrent tumors [3]. Furthermore, the molecular etiology of EOC remains unknown [4].

Autophagy is a lysosome-dependent degradation process that maintains cellular homeostasis by sequestering cytosolic components for degradation [5, 6]. It plays an important role in physiological processes such as growth, cell death, and aging, but its role in resistance against tumors remains controversial [7-9]. Autophagy commonly serves as a survival pathway that defends cells against stressors and enables them to overcome harsh conditions; these properties may contribute to tumor resistance and consequently to the development of anti-angiogenic therapy. However, it can be cytotoxic when the damage is critical [10, 11].

Circular RNAs (circRNAs) are formed from exons or introns through back-splicing and are characterized by covalently closed loop structures with high stability and resistance against RNA degradation [12, 13]. Accumulating evidence suggests that circRNAs play a role in various physiological functions by modulating alternative splicing, sponging microRNA, and regulating protein-RNA interactions and genes expression [14-16]. CircNRIP1 is a highly expressed circRNA in gastric cancer. Reportedly, silencing of CircNRIP1 inhibited its interaction with microRNA-149-5p and inhibited the progression of

gastric cancer via the AKT1/mTOR pathway [17]. Furthermore, overexpression of circRNA-3 (BCRC-3) was found to inhibit the proliferation of bladder cancer cells through sponging of miR-182-5p, which mediates the release of the inhibited P27 [18]. CircMUC16 was found to exacerbate EOC invasion and metastasis via interaction with ATG13 and miR-199a [19]. Interestingly, high expression levels of circCELSR1 contribute to paclitaxel resistance and progression of ovarian cancer. CircCELSR1 was found to act as a sponge by directly interacting with miR-1252, which further regulates FOXR2 expression [20]. According to a previous report, overexpression of circVPS13C in ovarian cancer cell lines is associated with tumor node and lymph node metastasis stage and promotes cell proliferation and invasion [21]. Furthermore, expression levels of circLARP4 are low in patients with ovarian cancer; therefore, this circRNA may serve as a potential biomarker of ovarian cancer prognosis [22].

Several circRNAs have been identified to be involved in the pathogenesis of EOC, but the underlying mechanisms need to be studied further. By conducting the RNA-seq analysis of autophagy model, we found that the expression of circEEF2 (hsa_circ_0048559) was significantly upregulated. Subsequently, we explored the effect of circEEF2 on autophagy, proliferation, and invasion in EOC and the potential mechanism involved.

Material and methods

Cell culture and transfection

Human ovarian cancer cell lines A2780 and SKOV3 were cultured in RPMI 1640 medium (Sigma-Aldrich, R8758) with 10% fetal bovine serum and 1% penicillin-streptomycin solution (Beyotime, C0222) in a 5% CO_2 incubator at 37°C. The following siRNA was used for silencing the target genes of human circEEF2, ATG5, and ATG7: CircEEF2-1: 5'-CCCCAUCAAGGCUGUGAUGTT-3'; CircEEF2-2: 5'-CAUCAAGGCUGUGAUGCGCTT-3'; ATG7: 5'-CAGUGGAUCUAAAUCUCAAACUGAU-3'; ATG5: 5'-CAAUCCCAUCCAGAGUUGCUUGUGA-3'. The following was used as a negative control (NC): 5'-UUCUUCGAAGGUGUCACGUTT-3'. Lentiviral vectors expressing shCircEEF2 or NC (circEEF2-LV2-1 and circEEF2-LV2-2 or circEEF2-LV2-NC) and that overexpressing circEEF2 or NC (circEEF2-LV6 or circEEF2-LV6-NC) were constructed by Genepharma (Shanghai China). The following is the sequence of miR-6881-3p mimics (Genepharma, Shanghai China): 5'-AUCCUCUUUCGUCCUUCCCACU-3'. Transfection reagent of siRNA mate plus was purchased from Genepharm, and the corresponding procedures were performed according to the manufacturer's instructions.

Cell proliferation assay

Cell proliferation was detected by using the Cell-Light™ EdU imaging detection kit (Ruibo Biotechnology, Guangzhou, China). In accordance with the manufacturer's instructions, ovarian cancer cells were seeded in 24-well plates. Subsequently, cells were incubated with 50 μM reagent A for 4 h, rinsed thrice with PBS, and fixed with 4% paraformaldehyde for 30 min. After a gentle rinse, cells were stained with Apollo 567 and Hoechst 33342 and photographed using a fluorescence microscope.

Invasion assays

Invasive abilities of SKOV3 and A2780 cells were detected using the invasion assay, which was conducted with transwell chambers (Corning, Inc., Lowell, MA, USA) containing a polycarbonate filter with an 8 μm pore size. Briefly, 500 μl complete medium was added to the 24-well plates outside the chamber. An equivalent of 5×10^4 cells was inoculated in the chamber and incubated with 200 μl basic medium at 37°C in 5% CO_2. After 48 h of incubation, the invasive cells on the opposite side of the filter were mildly rinsed with PBS, fixed with 4% paraformaldehyde, and stained with 0.5% crystal violet (Beyotime Institute of Biotechnology, C0121). After a complete rinse with PBS, the cells were photographed using the microscope.

Quantitative PCR assay

RNA was isolated from SKOV3 and A2780 cells using a Total RNA Rapid Extraction Kit (Bioteke Corporation, RP1201) in accordance with the manufacturer's instructions. Subsequently, the isolated RNA samples were quantified and used for synthesizing cDNA with circRNA fluorescence quantitative detection kit (Geneseed, GS0201, Guangzhou, China). The primers used in the study were synthesized by Sangon bio-

tech (Shanghai China). The primer sequences of circEEF2 are as follows: forward: 5'-ACCCCATGGTGCAGTGCATC-3' and reverse: 5'-AATGCCCATGGCAGCCTCGT-3'. The gene expression was quantified using the $2^{-\Delta\Delta CT}$ method.

Dual-luciferase reporter gene assay

SKOV3 cells were seeded into 24-well plates. Firstly, 100 nM miR-6881-3p or the control was transfected into cells and incubated for 24 h. Subsequently, 0.8 μg of corresponding vectors (ATG5-wt or mut, ATG7-wt or mut and CircEEF2-wt or mut) containing firefly luciferase and 1 μg renilla plasmid were co-transfected into SKOV3 cells transfected with miR-6881-3p or the control. After incubation for another 24 h, the relative luciferase activity was calculated by using the Dual-Luciferase Reporter Assay System (Promega Corporation, E1910) in accordance with the manufacturer's instruction. The Lipofectamine 2000 reagent (Invitrogen, Carlsbad, CA, USA) was used for transfection. The corresponding vectors were constructed by Genepharma (Shanghai China).

Western blotting (WB)

Total protein was isolated from cells using RIPA (Beyotime, P0013B)-containing PMSF (Beyotime, ST506). The extracted protein was separated using 10-15% SDS PAGE gel, transferred to a PVDF membrane, blocked with 5% milk, and incubated with the primary antibodies overnight at 4°C. After incubation with secondary antibody, proteins can be visualized using ECL Luminescent Solution. The primary antibodies included rabbit anti-ATG5 (CST, #12994), anti-ATG7 (CST, #8558), anti-ANXA2 (Abcam, ab41803), anti- p-mTOR (Abcam, ab109268), anti-P62 (CST, #5114), and anti-mTOR (Abcam, ab134903). Mouse anti-GAPDH (Proteintech, 1E6D9) was used as a normalized control.

RNA pulldown assay and matrix-assisted laser desorption/ionization time of flight mass spectrometry (MALDI-TOF-MS)

The proteins that were directly bound to circEEF2 were detected using the RNA pulldown assay, which was performed using Pierce™ Magnetic RNA-Protein Pull-Down Kit (Thermo Fisher, 20164) according to the manufacturer's instruction. The biotin-labeled probe for circEEF2 was purchased from Genepharma (Shanghai China). The pulled down protein was subjected to SDS-PAGE gel electrophoresis and silver staining (Fast Silver Stain Kit, Beyotime, P0017S). Subsequently, the differential bands were subjected to MALDI-TOF-MS to identify the specific proteins. mRFP-GFP-LC3 fluorescence monitor autophagy flux.

The autophagy double label system was introduced to track the autophagy flux. SKOV3 cells were stably infected with the lentiviral vectors expressing mRFP-GFP-LC3, shCircEEF2, or NC (circEEF2-LV2-1, circEEF2-LV2-2, or circEEF2-LV2-NC) while A2780 cells were stably infected with the lentiviral vectors expressing mRFP-GFP-LC3, circEEF2-LV6, or circEEF2-LV6-NC. LC3 dots were photographed using a confocal microscope and counted using image pro plus 6.0 software.

Fluorescence in situ hybridization (FISH) assay

Probes labeled with Cy3 and FAM for the detection of CircEEF2 and miR-6881-5p, respectively, were synthesized by Genepharma. Nuclei were stained with Hoechst 33342. FISH assay was performed according to the manufacturer's instructions (F03401, Genepharma). Finally, a confocal microscope was used for photographing.

In vivo tumor xenograft study

The animal experiments were approved by the Committee on the Use and Care on Animals (Chongqing Medical University, Chongqing, China) and conducted according to the institutional guidelines. The in vivo tumor proliferation effects were detected in 5 groups. Four-week-old BALB/c nude mice were subcutaneously inoculated with 5×10^6 (100 μL) SKOV3 cells stably infected with circ-EEF2-LV2-1/NC or 5×10^6 (100 μL) A2780 cells infected with circ-EEF2-LV6/NC. To detect whether chloroquine (CQ) could enhance the effect of silencing circEEF2, 50 mg/kg CQ was intraperitoneally (IP) injected every day for 3 weeks. The animals were sacrificed after 4 weeks, and established tumors were weighed. For the in vivo tumor metastasis studies, 4-week-old BALB/c nude mice were IP injected with 5×10^6 (200 μl) SKOV3 cells stably infected with circ-EEF2-LV2-1 or NC. The animals were sacrificed after

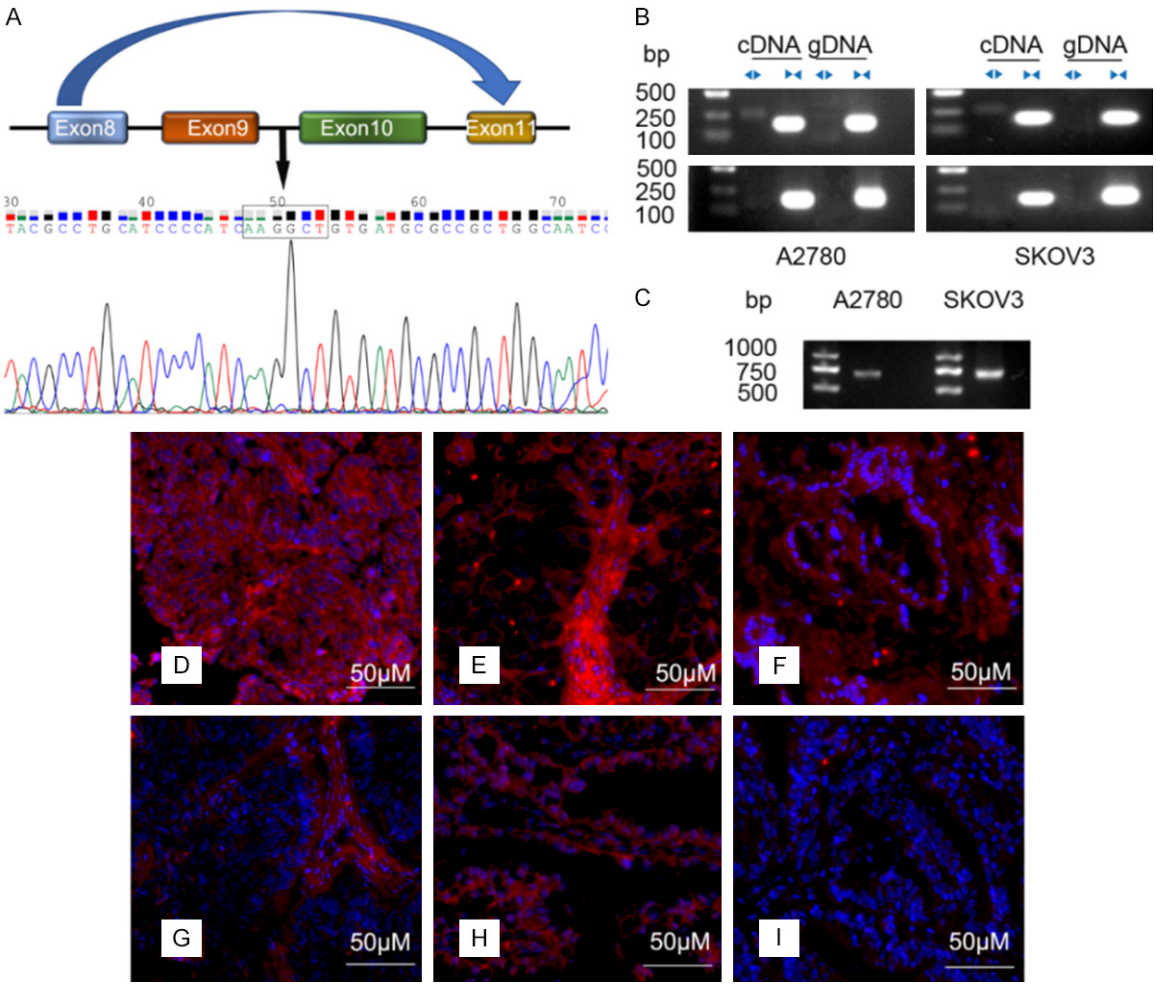

Figure 1. CircEEF2 is upregulated in the EOC tissue. A. Schematic illustration showing the circularization of EEF2 exon 8 to 11 forming circ-0048559 (circEEF2). Sanger sequencing showed the trans-splicing site of circEEF2. B. Agarose gel electrophoresis showed that circEEF2 could be amplified with the divergent primers and cDNA from SKOV3 and A2780 cells, but not with gDNA. C. Agarose gel electrophoresis showed that the length of circEEF2 is 702 bp. D. Serous carcinoma (stage IIIC). E. Clear cell carcinoma (stage IIIC). F. Mucinous carcinoma (stage IIIB). G. Serous carcinoma (stage IIB). H. Clear cell carcinoma (stage IIC). I. Normal ovarian tissue.

5 weeks to weigh the established tumors and to count and dissect the metastases.

Statistical analysis

All statistical analyses were performed using SPSS software, version 17.0 (Chicago, IL, USA). Data were obtained from three independent experiments and are presented as mean ± standard deviation (mean ± SD). The association between circEEF2 expression and clinicopathologic characteristics was analyzed by chi-squared test. Student's t-test was used for comparison between two groups. Statistical significance was defined as $P < 0.05$.

Results

CircEEF2 is upregulated in the EOC tissue

Based on the RNA-seq analysis of autophagy model, wherein autophagy was induced in SKOV3 cells by incubation with 10 μM torin1 for 24 h, we found that circEEF2 was significantly upregulated. As a novel circRNA, CircEEF2 has not been studied previously.

CircEEF2 originated from EEF2 pre-mRNA (exon 8, 9, 10, 11), whose spliced mature sequence length is 702 bp (**Figure 1A**, **1C**). Using Sanger sequencing technique, the trans-splicing site of circEEF2 was identified (**Figure**

Table 1. Association of circEEF2 expression with clinicopathological characteristics in 69 patients of EOC

Characteristics	NO. of patients (n = 69)	CircEEF2 Expression		*P* value
		Low no. (%)	High no. (%)	
Age (years)				> 0.05
< 50	26	11 (42.31%)	16 (57.69%)	
≥ 50	43	19 (44.19%)	24 (55.81%)	
Normal ovarian	12	8 (66.67%)	4 (33.33%)	
Cancer tissues	57	17 (29.82%)	32 (70.18%)	
Tumor type				< 0.05
clear cell carcinoma	8	2 (25.00%)	6 (75.00%)	
serous carcinoma	40	11 (27.5%)	29 (72.5%)	
mucinous scarcinoma	9	2 (22.22%)	7 (77.78%)	
FIGO stage				< 0.05
I/II	21	13 (61.90%)	8 (38.10%)	
III/IV	36	14 (38.89%)	22 (61.11%)	
Grade				
1	17	14 (82.35%)	3 (17.65%)	
2	18	11 (61.11%)	7 (38.89%)	
3	22	9 (40.91%)	13 (59.09%)	
		Grade 2-3 Versus 1		< 0.05

1A). Additionally, circEEF2 could be amplified using divergent primers and cDNA of SKOV3 and A2780 cells, but not and gDNA (**Figure 1B**). Hence, trans-splicing but not genomic rearrangements contributed to the head-to-tail splicing of circEEF2.

The expression of circEEF2 in tissue was examined using FISH. CircEEF2 was predominantly localized in the cytoplasm (**Figure 1D-I**). According to the tissue type of EOC (clear cell carcinoma, serous carcinoma, mucinous carcinoma), we found that circEEF2 was highly expressed in two-thirds of patients with this cancer type. Expression levels of CircEEF2 were high in EOC tissues but low in normal ovarian tissues ($P < 0.05$; **Table 1**). The expression of circEEF2 was higher in stage III/IV than in stage I/II ($P < 0.05$). Furthermore, the fluorescence intensity was correlated with the tumor grade (grades 2-3 vs. 1, $P < 0.05$). However, age distribution was not connected with circEEF2 expression ($P > 0.05$; **Table 1**).

CircEEF2 is implicated in autophagy

The basic expression levels of circEEF2 in EOC cell lines were detected using q-PCR. Expression levels of circEEF2 were the highest in SKOV3 cells but the lowest in A2780 cells (**Figure 2A**). Hence, SKOV3 and A2780 cells were used for the silencing and overexpression trials, respectively. The efficiency of ectopic expression or silencing was verified using q-PCR as shown in **Figure 2B** and **2C**. Autophagy but not apoptosis (data not show) was affected by silencing or ectopic expressing of circEEF2 in ovarian cancer cells. The expression of LC3-II decreased in the silencing trials involving LV2-1- or LV2-2-infected SKOV3 cells and increased in the ectopic expression trials involving LV6-infected A2780 cells; expression levels of P62 increased in the silencing group and decreased in the ectopic expression group (**Figure 2D**). To explore the reason behind the accumulation of LC3-II, the autophagosome formation inhibitor of 3-MA (3-methyladenine) or autophagosome-lysosome fusion inhibitor bafilomycin A1 (BafA1) were added to cells. Finally, 3-MA but not BafA1 reversed the LC3-II accumulation induced by the ectopic expression of circEEF2 (**Figure 2G**). These results indicate that the ectopic expression of circEEF2 interfered with the initiation but not maturation of autophagy. The effect of circEEF2 on autophagy flux was trucked by mRFP-GFP-LC3 reporter. The red puncta representing LC3 in-

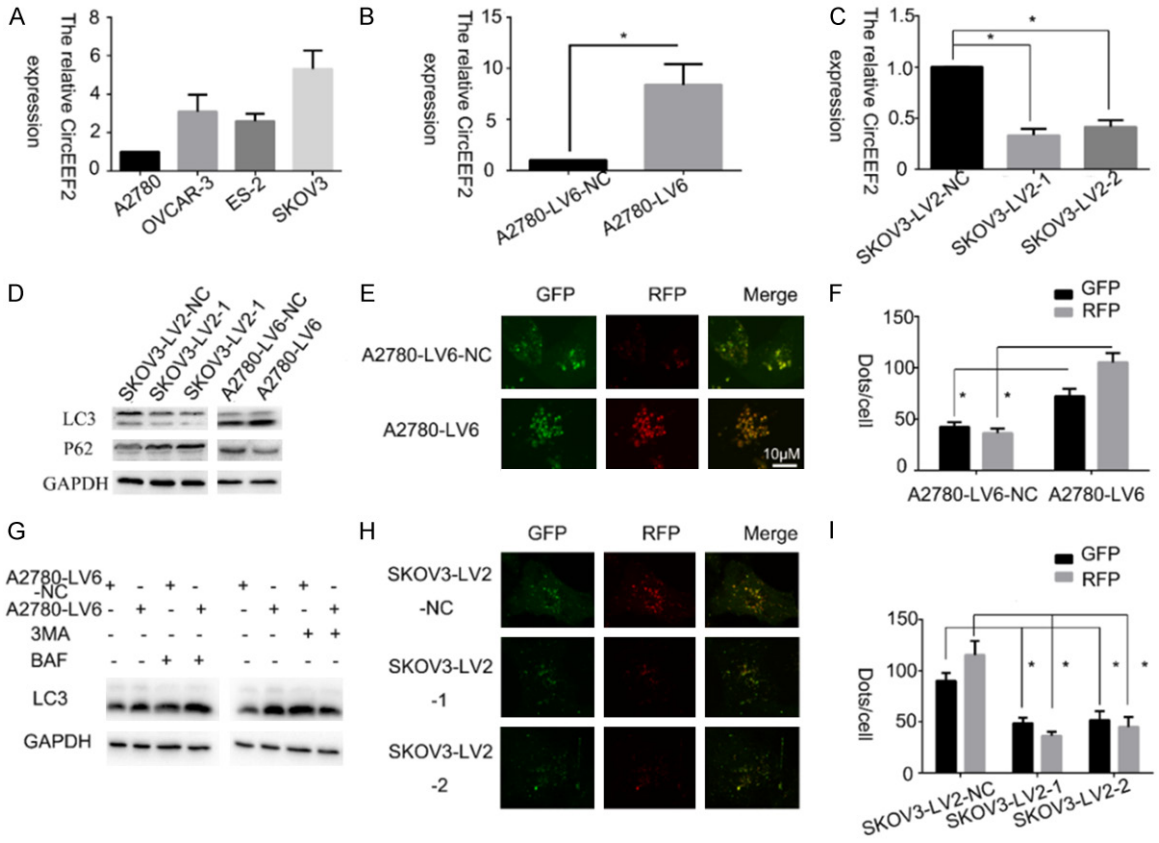

Figure 2. CircEEF2 is implicated in autophagy. A. Basic expression of cirEEF2 was detected in EOC cell lines by qPCR. B. Efficiency of overexpression of circEEF2 in A2780 cells was detected using qPCR. C. Efficiency of silencing of circEEF2 in SKOV3 cells was detected using qPCR. D. Expression of LC3-II and P62 was detected by Western blotting (WB) after the silencing or overexpression of circEEF2. E and F or H and I. Autophagy flux tracked by mRFP-GFP-LC3 fluorescence was analyzed by confocal microscopy after overexpression or silencing of circEEF2. The symbol * represented $P < 0.05$. Scale bar: 10 μm. G. Expression of LC3-II was detected by WB after adding autophagy blockers 3-MA or Baf.

creased in A2780-LV6 and decreased in SKOV3-LV2-1 and SKOV3-LV2-2 (**Figure 2E** and **2F**, **2H** and **2I**). These results indicate that circEEF2 ectopic expression activated autophagy.

CircEEF2 mediated autophagy promoted cellular proliferation and invasion

The role of autophagy in tumor growth is controversial: it is not clear whether it promotes or inhibits tumor growth. Thus, the effect of autophagy induced by the ectopic expression of circEEF2 on cellular proliferation and invasion were detected. Our data shows that the proliferation and invasion ability increase when circEEF2 is overexpressed in A2780 cells. This effect could be partly reversed by silencing ATG5 or ATG7 (**Figure 3A** and **3B**). Hence, circEEF2 promotes the proliferation and invasion in ovarian cancer cells, which were related with autophagy.

CircEEF2 promoted autophagy by sponging miR-6881-3p

The differential miRNAs of mir-3147, mir-6721-5p, mir-6881-3p, and mir-597-3p was predicted by bioinformatics analysis (Miranda v3.3a). Ectopic expression of circEEF2 significantly decreased the expression of miR-6881-3p (**Figure 4A**). Bioinformatics prediction (targetscan human 7.2) shows ATG5 and ATG7 as the potential targets of miR-6881-3p (**Figure 4E**). The direct interactions among circEEF2, miR-6881-3p, ATG5, and ATG7 were confirmed by Dual-luciferase reporter gene assay (**Figure 4B-D**). Further, FISH assay demonstrated that circEEF2 and miR-6881-3p were overlapped and mainly co-localized in the cyto-

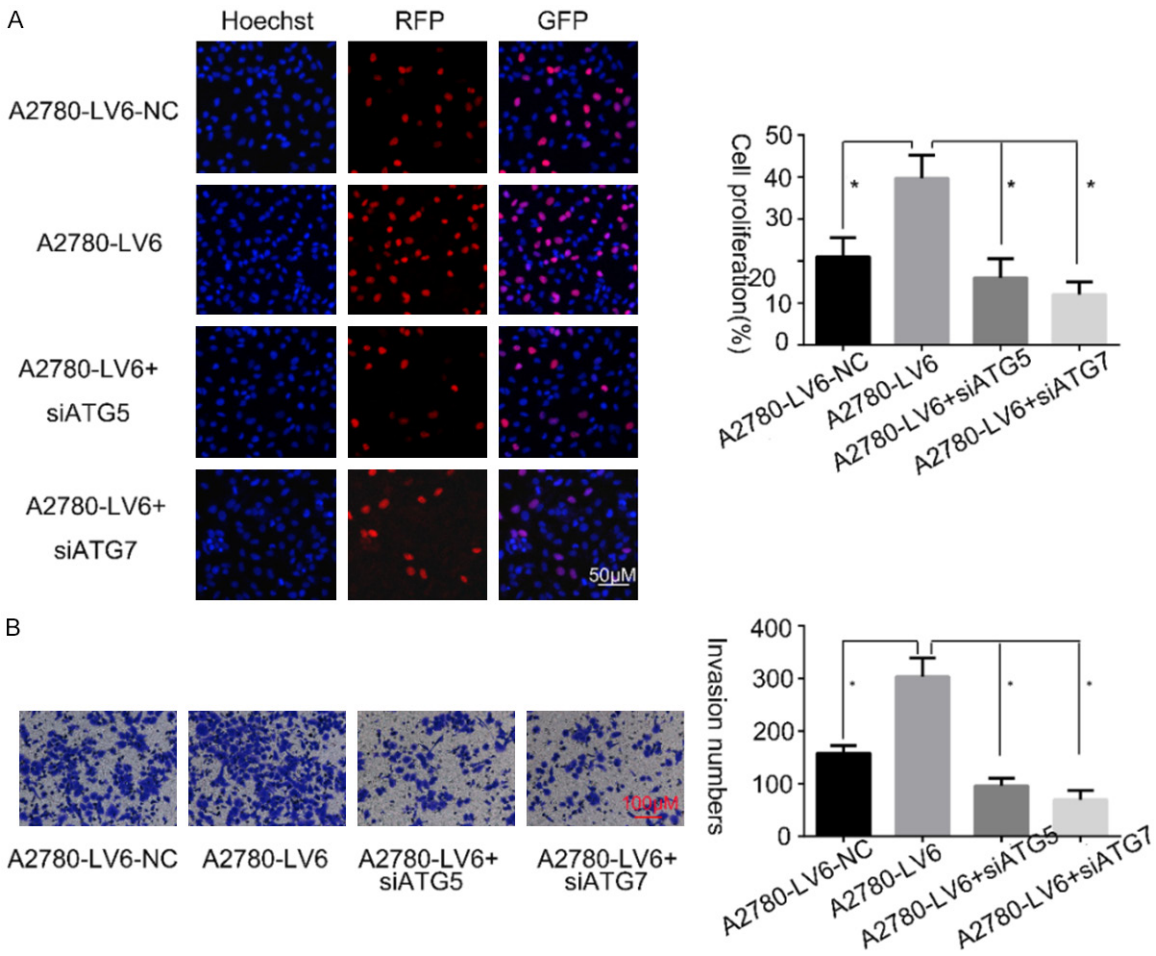

Figure 3. CircEEF2-facilitated cellular proliferation and invasion were related to autophagy. A. Using EdU assay, proliferation was detected after overexpression of circEEF2 or after silencing ATG7 or ATG5 in A2780. The specific groups were as follows: A2780-NC, A2780-LV6, A2780-LV6 + siATG5, and A2780-LV6 + siATG7. Original magnification, 200 ×, Scale bar: 50 μm. B. After silencing ATG5 or ATG7 in A2780 cells and stably overexpressing circEEF2 for 48 h, the invasion assays were performed. The specific groups were as follows: A2780-NC, A2780-LV6, A2780-LV6 + siATG5, and A2780-LV6 + siATG7. Error bars represent standard error. * represented $P < 0.05$. Scale bar: 100 μm.

plasm (**Figure 4F**). The expressions of ATG5 and ATG7 were inhibited after silencing circEEF2 in SKOV3 cells and increased in A2780 cells after ectopic expression of circEEF2 (**Figure 5A**). Ectopic expression of miR-6881-3p decreased the expression of ATG5 and ATG7 (**Figure 5D**). Ectopic expression of circEEF2 increased LC3-II abundance, which was reduced by silencing ATG5 or ATG7 or by the ectopic expression of miR-6881-3p (**Figure 5E**). Consistently, the autophagy fluxs stimulated by circEEF2 was partially rescued via silencing of ATG5 or ATG7 or via ectopic expression of miR-6881-3p (**Figure 5B**, **5G**). Notably, ATG5 and ATG7 are autophagy markers. Hence, the data indicated that circEEF2 promoted autophagy by sponging miR-6881-3p. We further detected the effects of overexpression of miR-6881-3p on cellular proliferation and migration. Ectopic expression of circEEF2 promoted proliferation and migration. The effect was partially reversed by the overexpression of miR-6881-3p and silencing of ATG5 or ATG7 (**Figure 5C**, **5F**, **5H**, **5I**).

CircEEF2 directly binds to ANXA2

RNA pulldown assay was performed to identify the proteins the directly bind with circEEF2. The proteins pulled were separating by using SDS-PAGE gel electrophoresis. After silver staining, the differential bands were observed (red box)

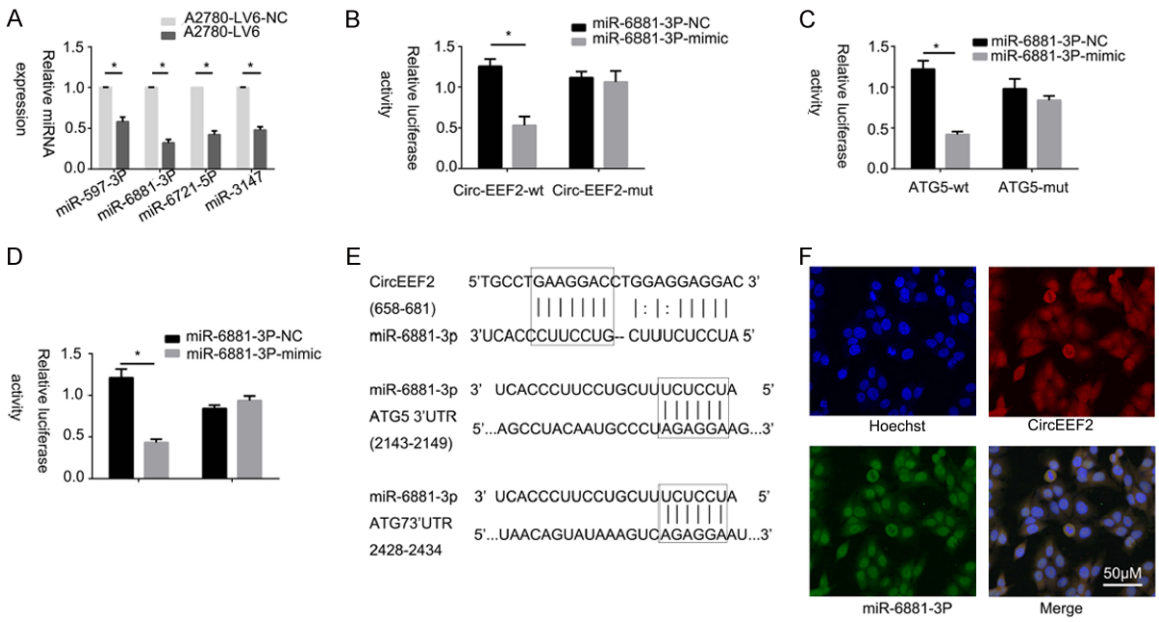

Figure 4. Sponging of miR-6881-3p by circEEF2. A. Predicted miRNAs expression was verified by qPCR in A2780 cells that stably overexpressed circEEF2. B-D. SKOV3 cells were transfected with miR-6881-3P mimic or NC, which was followed by co-transfection with corresponding vectors (ATG5-wt or mut, ATG7-wt or mut, and CircEEF2-wt or mut) containing firefly luciferase and renilla plasmid. Luciferase activity was measured. Error bars represent the standard error. The symbol * represents $P < 0.05$. E. Binding site predicted by bioinformatics analysis. F. Colocalization of miR-6881-3p and circEEF2 was detected using FISH assay and photographed by confocal microscope in SKOV3 cells. Scale bar: 50 μm.

(**Figure 6A**). Two peptides of ANXA2 named QDLAFAYQRR and DALNIETAIK were identified by using MALDI-TOF-MS, WB assay further proved that ANXA2 could be pulled down (**Figure 6B**, **6C**). It indicated that circEEF2 directly binds to ANXA2. The potential binding sites between circEEF2 and ANXA2 were predicted by catRAPID (**Figure 6F**). The Δ239-290 region of ANXA2 directly bound to cirEEF2 (**Figure 6G**). A previous study reported that ANXA2 regulated autophagy by regulating the Akt1-mTOR-ULK1/2 signaling pathway [23]. Therefore, we speculated that circEEF2 binds to ANXA2 and prompts autophagy. Silencing circEEF2 inhibited the expression of ANXA2 and promoted that of p-MOR, while ectopic expression of circEEF2 promoted the expression of ANXA2 and inhibited that of p-MOR; the expression of mTOR was not affected in either of the scenarios (**Figure 6D**). Furthermore, the relationship between ANXA2 expression and overall survival (OS) of the ovarian cancer patients was analyzed by using TCGA online tool (http://gepia.cancer-pku.cn/). We found that low expression levels of ANXA2 mRNA were significantly related to OS of patients with ovarian cancer (**Figure 6E**).

CircEEF2 promoted xenograft tumor growth and mediated metastasis in vivo

We further examined the role of circEEF2 in tumor formation using an animal model. CircEEF2-silencing decreased the average weight and volume of tumors. This effect was further amplified by CQ. Conversely, up-regulation of circEEF2 increased the average weight and volume of tumors (**Figure 7A**, **7C-F**). The expression of ATG5, ATG7, and ANXA2 decreased in the circEEF2-silencing group and increased in circEEF2-overexpression group (**Figure 7B**). Silencing circEEF2 reduced the average weight of the metastases (**Figure 7G**, **7H**). These data show that silencing circEEF2 inhibited metastasis in vivo. Based on the above-mentioned findings, we speculated that circEEF2 promoted autophagy in EOC via two paths: circEEF2 directly interacted with miR-6881-3p to increase the expression of ATG5 and ATG7; circEEF2 binds directly to ANXA2 to inhibit the activation of p-mTOR (**Figure 7I**).

Discussion

In the present study, the expression of circEEF2 was observed to be higher in EOC tissues than

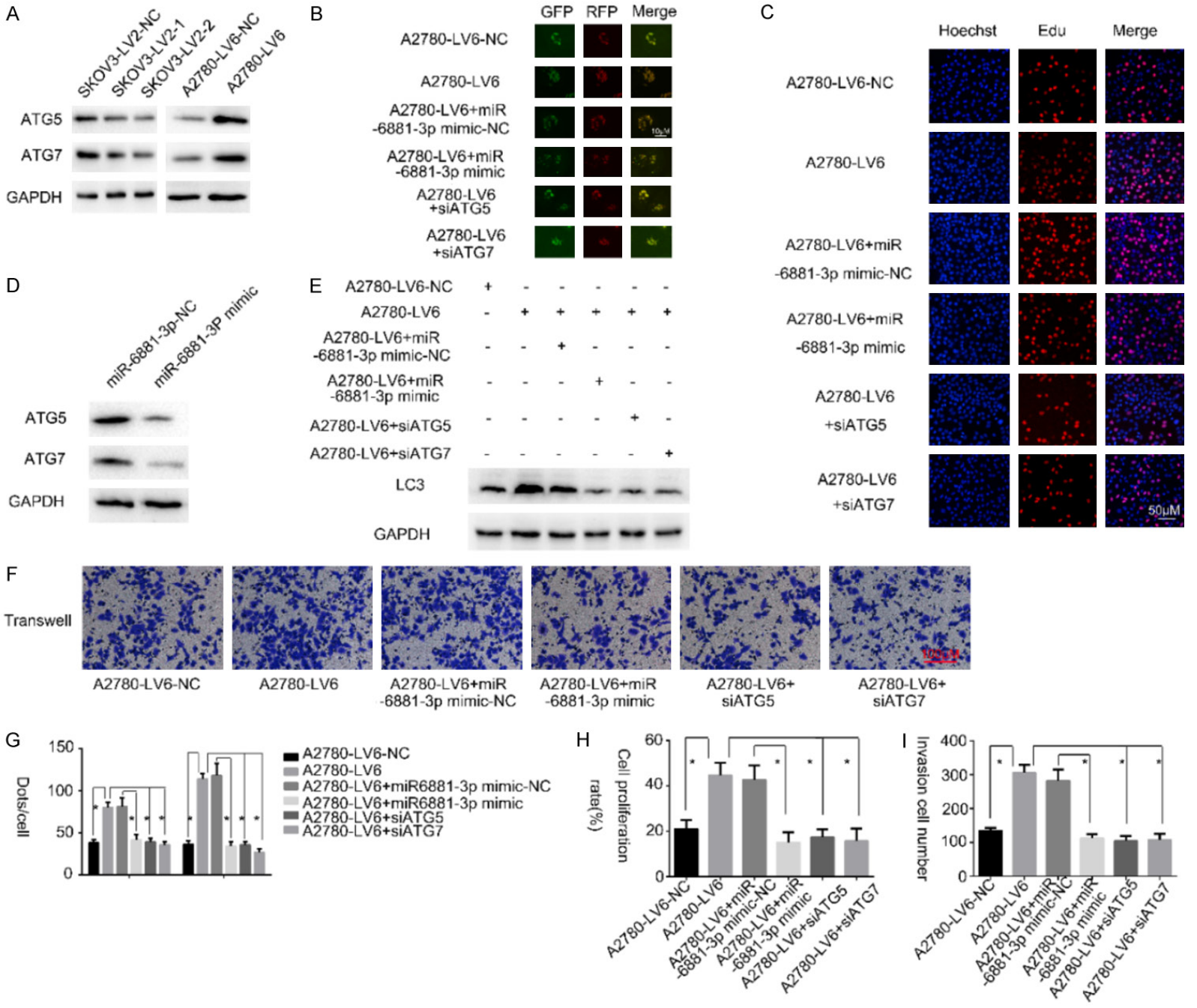
A
SKOV3-LV2-NC
SKOV3-LV2-1
SKOV3-LV2-2
A2780-LV6-NC
A2780-LV6
ATG5
ATG7
GAPDH
B
GFP
RFP
Merge
A2780-LV6-NC
A2780-LV6
A2780-LV6+miR -6881-3p mimic-NC
A2780-LV6+miR -6881-3p mimic
A2780-LV6 +siATG5
A2780-LV6 +siATG7
C
Hoechst
Edu
Merge
A2780-LV6-NC
A2780-LV6
A2780-LV6+miR -6881-3p mimic-NC
A2780-LV6+miR -6881-3p mimic
A2780-LV6 +siATG5
A2780-LV6 +siATG7
50μM
D
miR-6881-3p-NC
miR-6881-3P mimic
ATG5
ATG7
GAPDH
E
A2780-LV6-NC
A2780-LV6
A2780-LV6+miR -6881-3p mimic-NC
A2780-LV6+miR -6881-3p mimic
A2780-LV6+siATG5
A2780-LV6+siATG7
LC3
GAPDH
F
Transwell
A2780-LV6-NC
A2780-LV6
A2780-LV6+miR -6881-3p mimic-NC
A2780-LV6+miR -6881-3p mimic
A2780-LV6+ siATG5
A2780-LV6+ siATG7
G
Dots/cell
A2780-LV6-NC
A2780-LV6
A2780-LV6+miR6881-3p mimic-NC
A2780-LV6+miR6881-3p mimic
A2780-LV6+siATG5
A2780-LV6+siATG7
H
Cell proliferation rate(%)
A2780-LV6-NC
A2780-LV6
A2780-LV6+miR -6881-3p mimic-NC
A2780-LV6+miR -6881-3p mimic
A2780-LV6+siATG5
A2780-LV6+siATG7
I
Invasion cell number
A2780-LV6-NC
A2780-LV6
A2780-LV6+miR -6881-3p mimic-NC
A2780-LV6+miR -6881-3p mimic
A2780-LV6+siATG5
A2780-LV6+siATG7

Figure 5. CircEEF2 promoted autophagy by regulating miR-6881-3p/ATG5/ATG7 axis. A. Expression levels of ATG5 and ATG7 were detected using Western blotting (WB) after overexpression or knockdown of circEEF2 in A2780 or SKOV3 cells. B and G. Autophagy flux was tracked in the following groups using mRFP-GFP-LC3 fluorescence and confocal microscopy: A2780-NC, A2780-LV6, A2780-LV6 + miR-6881-3P-mimic-NC, A2780-LV6 + miR-6881-3P-mimic, A2780-LV6 + siATG5, and A2780-LV6 + siATG7. Error bars represent the standard error. The symbol * represents $P < 0.05$. Scale bar: 10 μm. C and H. Cell proliferation was assessed using EdU assay. Original magnification, 200 ×, Scale bar: 50 μm. D. Expression levels of ATG5 and ATG7 in A2780 cells transfected with miR-6881-3p mimic or miR-6881-3p mimic-NC were detected using Western blotting (WB). E. Expression level of LC3-II was detected using WB in the following groups: A2780-NC, A2780-LV6, A2780-LV6 + miR-6881-3P-mimic-NC, A2780-LV6 + miR-6881-3P-mimic, A2780-LV6 + siATG5, and A2780-LV6 + siATG7. F and I. Invasion assays were performed after transfection for 48 h. Error bars represent standard error. * represents $P < 0.05$. Scale bar: 100 μm.

in normal control. The expression of circEEF2 was related to the grade and FIGO stage of EOC. In addition, the upregulation of circEEF2 facilitated proliferation, invasion, and autophagy in EOC cells. CircEEF2 regulated the expression of ATG5 or ATG7 by sponging miR-6881-3p. Furthermore, circEEF2 could directly bind to ANXA2. Therefore, circEEF2 may serve as a potential biomarker for EOC.

Autophagy plays a pivotal role in maintaining the normal functions of proteins and organelles as well as in energy homeostasis [5, 6]. It serves an intricate and paradoxical role in tumors. PTEN and TSC1/2 act as tumor suppressors by promoting autophagy via negative regulation of the protein kinase mTOR [24-29]. MARCH5 promotes migration, invasion, and autophagy of EOC [30]. ALKBH5, acts as a tumor-promoted gene by inhibiting autophagy via regulation of the ERK/MAPK and PI3K/AKT/mTOR pathways [31]. In this study, circEEF2 promoted EOC proliferation, migration, and autophagy. Based on the stimulus and cell system, autophagy can act as a pro-survival or pro-death factor [32, 33]. A previous study showed that the knockdown of circRACGAP1 sensitizes gastric cancer cells to apatinib via autophagy inhibition in vitro and in vivo [34]. Furthermore, down-regulation of OGT in ovarian cancer cells was found to contribute to cisplatin resistance by inducing autophagy [35]. Silencing BRCA2 enhanced autophagy in EOC cells. Autophagy inhibitor CQ reportedly further sensitizes cells to the action of CDDP in BRCA2-silenced cells [36]. In this study, we found that the inhibition of autophagy by CQ or silencing of ATG5 or ATG7 could reverse the pro-survival function of circEEF2 in EOC cells. In vivo trials combining circEEF2-silencing with CQ further inhibited the proliferation and migration of cancer cells.

The roles of circRNAs have been identified in many cancer types, including EOC. They typically regulate the target genes by sponging miRNAs. Circ-SOX4 was found to expedite lung adenocarcinoma by sponging miR-1270 and activating the WNT signaling pathway [37]. The overexpression of circ_LARP4 was found to suppress the proliferation and migration of ovarian cancer cells by interacting with miR-513b-5p to regulate the expression of LARP4 [38]. Reportedly, circPUM1 directly interacts with miR-615-5p and miR-6753-5p to promote the development of ovarian cancer [39]. In this study, circEEF2 was not involved in apoptosis but promoted autophagy. ATG5 and ATG7 are two pivotal molecules that promote autophagy. miR-6881-3p inhibited autophagy by targeting ATG5 and ATG7. CircEEF2 directly bound to and down-regulated miR-6881-3p. Our findings revealed that circEEF2 regulated ATG5 and ATG7 by sponging miR-3185.

Epithelial-mesenchymal transition (EMT) has been illustrated as a key mechanism of metastasis [40]. In a previous study, down-regulation of Anxa2 inhibited EMT and attenuated the proliferation and invasion of ovarian cancer cells [41]. Another study showed that Anxa2 promoted NSCLC cell EMT via increasing the expression of EMT-driver transcription factor of snail and further contributed to the invasion by inhibiting p53 signaling. Knockdown of Anxa2 was found to inhibit cell proliferation [42]. Furthermore, Anxa2 was involved in inducing cisplatin and vincristine resistance in gastric cancer cells [43]. Hence, Anxa2 plays a pivotal role in tumor progression and chemotherapy resistance. In this study, circEEF2 directly bound to Anxa2 and regulated its expression. CircEEF2 affected ovarian cancer progression by regulating autophagy. Previous studies suggested that Anxa2 regulated autophagy by regulating the Akt1-mTOR-ULK1/2 signaling pathway [23]. CircEEF2 directly bound to Anxa2 to regulate autophagy in EOC. In summary, the present study demonstrated that circEEF2 was correlated with the tumor FIGO stage and

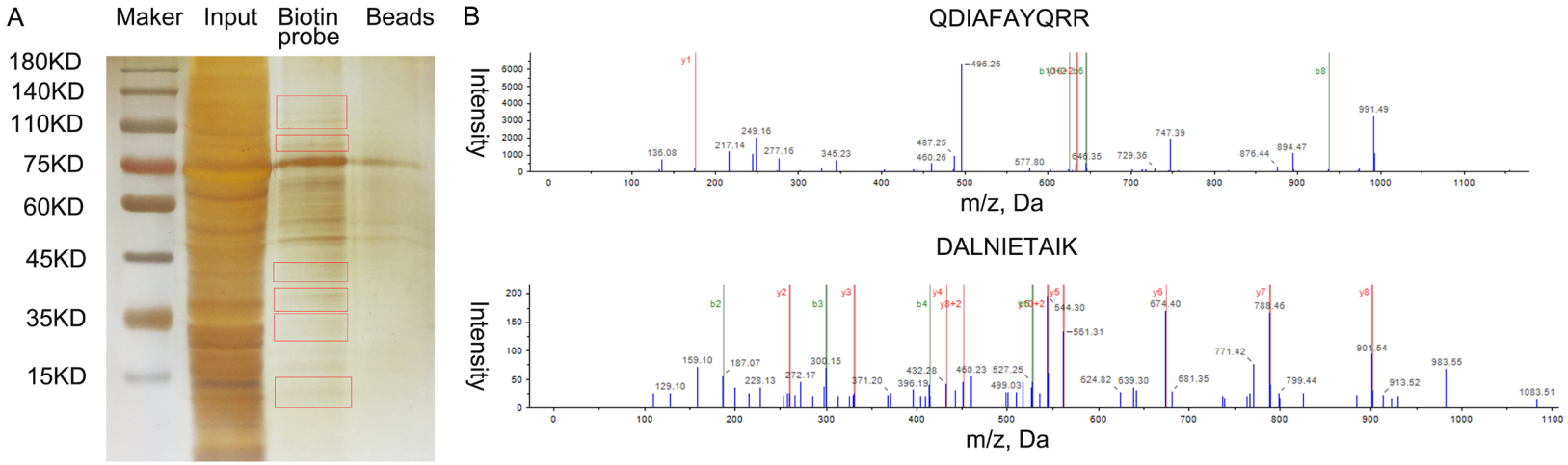

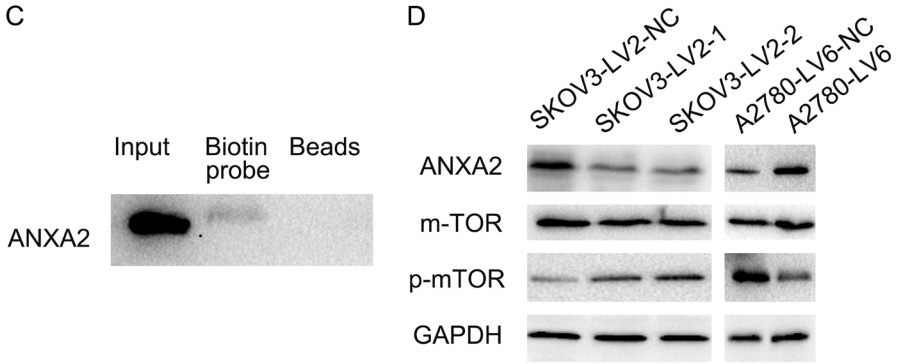

Figure 6. CircEEF2 directly binds to ANXA2. A. Silver staining revealed differential bands (in red box) obtained through circEEF2 RNA pull-down assay. B. Two peptides named QDIAFAYQRR and DALNIETAIK of ANXA2 were identified by MALDI-TOF-MS. C. ANXA2 was detected by Western blotting (WB) after circEEF2 RNA pulldown assay. D. Expression levels of ANXA2, p-MTOR, and m-TOR were determined using WB after knockdown or overexpression of circEEF2 in SKOV3 or A2780 cells. E. Relationship between ANXA2 expression and overall survival was analyzed in patients with ovarian cancer based on TCGA data. F. Potential interaction sites between circEEF2 and ANXA2 were predicted via catRAPID. G. PCMV5 vector containing ANXA2 DNA segments (PCMV5 vector, PCMV5-ANXA2, PCMV5-Δ139-190, PCMV5-Δ239-290 or PCMV5-Δ251–302) were used to transfect in SKOV3 cells for 48 h. Expression of circEEF2 was detected using q-PCR. Error bars represent the standard error. The symbol * indicates $P < 0.05$.

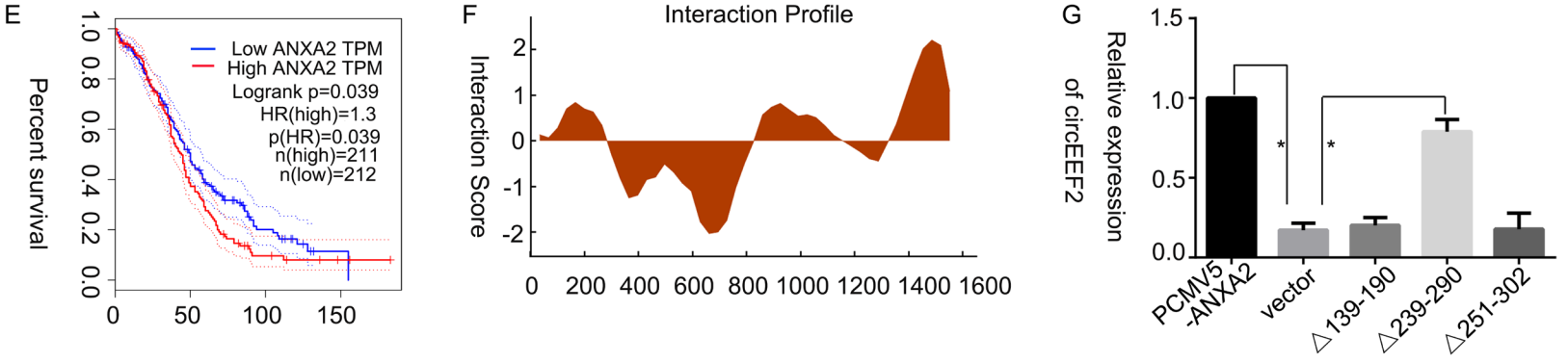

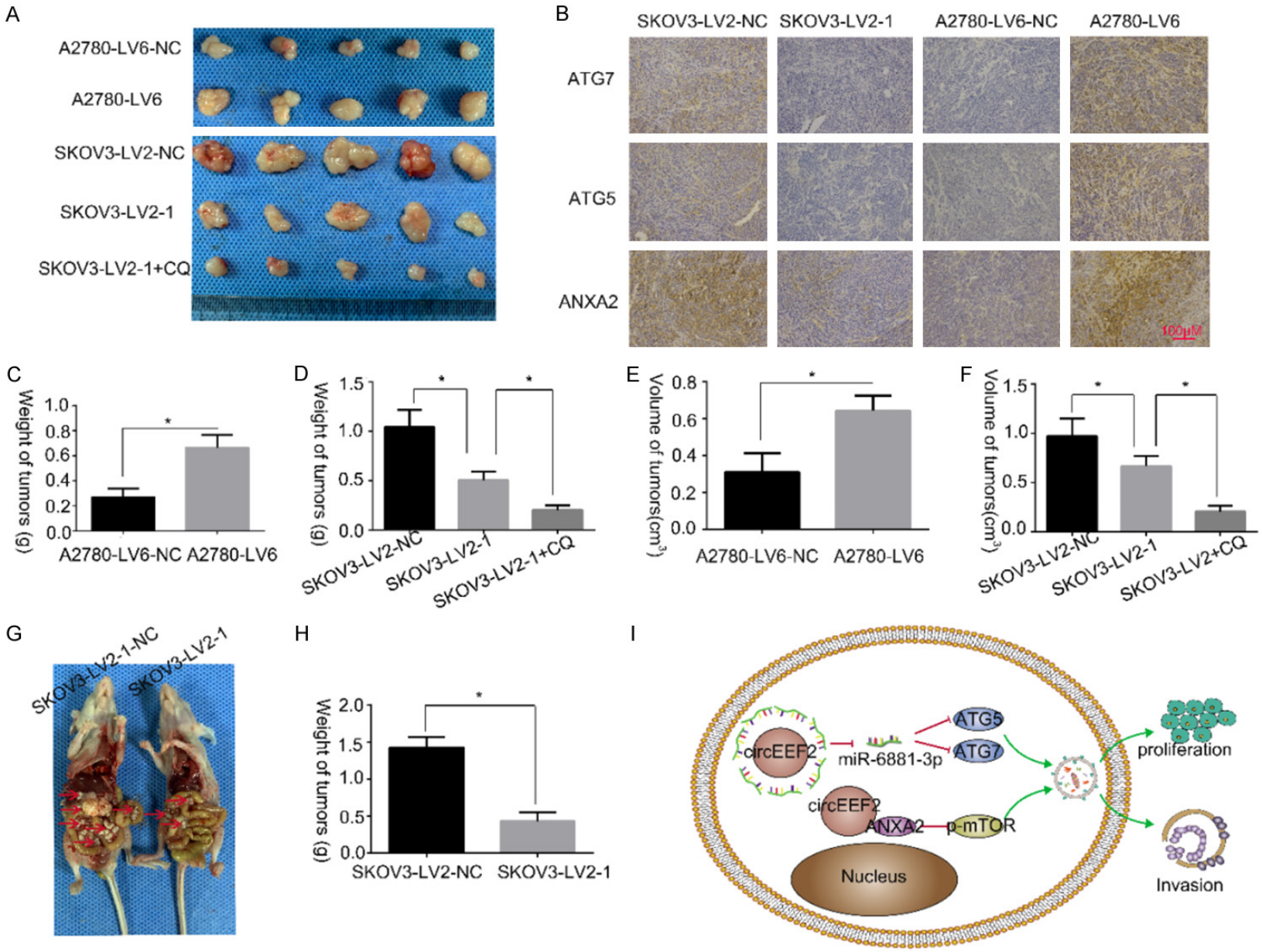
A
A2780-LV6-NC
A2780-LV6
SKOV3-LV2-NC
SKOV3-LV2-1
SKOV3-LV2-1+CQ
B
SKOV3-LV2-NC
SKOV3-LV2-1
A2780-LV6-NC
A2780-LV6
ATG7
ATG5
ANXA2
100μM
C
Weight of tumors (g)
A2780-LV6-NC
A2780-LV6
D
Weight of tumors (g)
SKOV3-LV2-NC
SKOV3-LV2-1
SKOV3-LV2-1+CQ
E
Volume of tumors(cm3)
A2780-LV6-NC
A2780-LV6
F
Volume of tumors(cm3)
SKOV3-LV2-NC
SKOV3-LV2-1
SKOV3-LV2+CQ
G
SKOV3-LV2-1-NC
SKOV3-LV2-1
H
Weight of tumors (g)
SKOV3-LV2-NC
SKOV3-LV2-1
I
circEEF2
miR-6881-3p
ATG5
ATG7
proliferation
circEEF2
ANXA2
p-mTOR
Nucleus
Invasion

Figure 7. CircEEF2 promoted xenograft tumor growth and mediated metastasis in vivo. A and C-F. After 4 weeks of tumor cell injection, xenograft tumors of each groups were isolated and photographed. The mean tumor volume and weight were measured. *represented $P < 0.05$. B. IHC of ATG5, ATG7, and ANXA2 expressions were analyzed on xenograft tumors. Original magnification: 200 ×, Scale bar: 100 μm. G. Silencing circEEF2 suppressed EOC proliferation and invasion in the pelvis, as observed using abdominal the metastasis model. The arrow indicates the tumor in the abdominal cavity. H. After 5 weeks of intraperitoneal tumor cell injection, the mean tumor weight was measured. I. A graphic abstract depicting the circEEF2 pathway (CircEEF2, ANXA2, ATG5, ATG7, and miR-6881-3P).

grade. CircEEF2-mediated autophagy facilitated the proliferation and invasion of EOC. CircEEF2-silencing combined with CQ further inhibited the tumor proliferation. Hence, CircEEF2 may be used as a potential target and biomarker for ovarian cancer.

Acknowledgements

We thank for the help offered by the Chongqing Key Laboratory of Obstetrics and Gynecology and Joint International Research Lab for Reproduction and Development, Ministry of Education. This study was supported by the National Science Foundation of China (81702557), the Nanchong City-School Science and Technology Strategic Cooperation Project (19-SXHZ0293), the Key Scientific Research Project of North Sichuan Medical College (CBY18-A-ZD21), the Scientific Research Project of Affiliated Hospital of North Sichuan Medical College (2020JC021).

Disclosure of conflict of interest

None.

Address correspondence to: Lina Hu, Department of Obstetrics and Gynecology, Second Affiliated Hospital, Chongqing Medical University, Linjiang Road, No. 76, Chongqing 400010, China. E-mail: 302502@hospital.cqmu.edu.cn

References

[1] Jemal A, Siegel R, Xu J and Ward E. Cancer statistics, 2010. CA Cancer J Clin 2010; 60: 277-300.

[2] Shih KK and Chi DS. Maximal cytoreductive effort in epithelial ovarian cancer surgery. J Gynecol Oncol 2010; 21: 75-80.

[3] Ozols RF. Recurrent ovarian cancer: evidence-based treatment. J Clin Oncol 2002; 20: 1161-1163.

[4] Reade CJ, McVey RM, Tone AA, Finlayson SJ, McAlpine JN, Fung-Kee-Fung M and Ferguson SE. The fallopian tube as the origin of high grade serous ovarian cancer: review of a paradigm shift. J Obstet Gynaecol Can 2014; 36: 133-140.

[5] Talukdar S, Pradhan AK, Bhoopathi P, Shen XN, August LA, Windle JJ, Sarkar D, Furnari FB, Cavenee WK, Das SK, Emdad L and Fisher PB. Regulation of protective autophagy in anoikis-resistant glioma stem cells by SDCBP/MDA-9/Syntenin. Autophagy 2018; 14: 1845-1846.

[6] Klionsky DJ. Why do we need to regulate autophagy (and how can we do it)? A cartoon depiction. Autophagy 2018; 14: 1661-1664.

[7] Vantaggiato C, Panzeri E, Castelli M, Citterio A, Arnoldi A, Santorelli FM, Liguori R, Scarlato M, Musumeci O, Toscano A, Clementi E and Bassi MT. ZFYVE26/SPASTIZIN and SPG11/SPATACSIN mutations in hereditary spastic paraplegia types AR-SPG15 and AR-SPG11 have different effects on autophagy and endocytosis. Autophagy 2019; 15: 34-57.

[8] Kim BW, Jin Y, Kim J, Kim JH, Jung J, Kang S, Kim IY, Kim J, Cheong H and Song HK. The C-terminal region of ATG101 bridges ULK1 and PtdIns3K complex in autophagy initiation. Autophagy 2018; 14: 2104-2116.

[9] Urano Y, Mori C, Fuji A, Konno K, Yamamoto T, Yashirogi S, Ando M, Saito Y and Noguchi N. 6-Hydroxydopamine induces secretion of PARK7/DJ-1 via autophagy-based unconventional secretory pathway. Autophagy 2018; 14: 1943-1958.

[10] Fan J, Liu YW, Yin J, Li QQ, Li YM, Gu J, Cai WH and Yin GY. Oxygen-glucose-deprivation/reoxygenation-induced autophagic cell death depends on JNK-mediated phosphorylation of Bcl-2. Cell Physiol Biochem 2016; 38: 1063-1074.

[11] Arun B, Akar U, Gutierrez-Barrera AM, Hortobagyi GN and Ozpolat B. The PARP inhibitor AZD2281 (Olaparib) induces autophagy/mitophagy in BRCA1 and BRCA2 mutant breast cancer cells. Int J Oncol 2015; 47: 262-268.

[12] Chen Y, Wei SZ, Wang XY, Zhu XL and Han SH. Progress in research on the role of circular RNAs in lung cancer. World J Surg Oncol 2018; 16: 215.

[13] Holdt LM, Kohlmaier A and Teupser D. Circular RNAs as therapeutic agents and targets. Front Physiol 2018; 9: 1262.

[14] Li ZY, Huang C, Bao C, Chen L, Lin M, Wang XL, Zhong GL, Yu B, Hu WC, Dai LM, Zhu PF, Chang ZX, Wu QF, Zhao Y, Jia Y, Xu P, Liu HJ and Shan

G. Exon-intron circular RNAs regulate transcription in the nucleus. Nat Struct Mol Biol 2015; 22: 256-264.
[15] Hansen TB, Jensen TI, Clausen BH, Bramsen JB, Finsen B, Damgaard CK and Kjems J. Natural RNA circles function as efficient microRNA sponges. Nature 2013; 495: 384-388.
[16] Granados-Riveron JT and Aquino-Jarquin G. The complexity of the translation ability of circRNAs. Bba-Gene Regul Mech 2016; 1859: 1245-1251.
[17] Zhang X, Wang S, Wang HX, Cao JC, Huang XX, Chen Z, Xu PH, Sun GL, Xu JH, Lv JL and Xu ZK. Circular RNA circNRIP1 acts as a microRNA-149-5p sponge to promote gastric cancer progression via the AKT1/mTOR pathway. Mol Cancer 2019; 18: 20.
[18] Xie F, Li YW, Wang M, Huang C, Tao D, Zheng FX, Zhang H, Zeng FQ, Xiao XY and Jiang GS. Circular RNA BCRC-3 suppresses bladder cancer proliferation through miR-182-5p/p27 axis. Mol Cancer 2018; 17: 144.
[19] Gan XL, Zhu HT, Jiang XW, Obiegbusi SC, Yong M, Long XT and Hu JG. CircMUC16 promotes autophagy of epithelial ovarian cancer via interaction with ATG13 and miR-199a. Mol Cancer 2020; 19: 45.
[20] Zhang S, Cheng J, Quan CL, Wen H, Feng Z, Hu Q, Zhu J, Huang Y and Wu XH. circCELSR1 (hsa(-)circ(-)0063809) contributes to paclitaxel resistance of ovarian cancer cells by regulating FOXR2 expression via miR-1252. Mol Ther-Nucl Acids 2020; 19: 718-730.
[21] Bao LP, Zhong JX and Pang LJ. Upregulation of circular RNA VPS13C-has-circ-001567 promotes ovarian cancer cell proliferation and invasion. Cancer Biother Radio 2019; 34: 110-118.
[22] Zou T, Wang PL, Gao Y, Liang WT. Circular RNA_LARP4 is lower expressed and serves as a potential biomarker of ovarian cancer prognosis. Eur Rev Med Pharmaco 2018; 22: 7178-7182.
[23] Li RP, Tan SR, Yu M, Jundt MC, Zhang S and Wu M. Annexin A2 regulates autophagy in pseudomonas aeruginosa infection through the Akt1-mTOR-ULK1/2 signaling pathway. J Immunol 2015; 195: 3901-3911.
[24] Zhang YJ, Fan YZ, Huang SK, Wang GY, Han R, Lei FX, Luo AQ, Jing X, Zhao L, Gu SZ and Zhao XH. Thymoquinone inhibits the metastasis of renal cell cancer cells by inducing autophagy via AMPK/mTOR signaling pathway. Cancer Sci 2018; 109: 3865-3873.
[25] Xin XR, Wu MY, Meng QY, Wang C, Lu YA, Yang YX, Li XN, Zheng QD, Pu H, Gui X, Li TM, Li J, Jia S and Lu DD. Long noncoding RNA HULC accelerates liver cancer by inhibiting PTEN via autophagy cooperation to miR15a. Mol Cancer 2018; 17: 94.
[26] Wang X, Li Y, Fan Y, Yu XM, Mao XY and Jin F. PTBP1 promotes the growth of breast cancer cells through the PTEN/Akt pathway and autophagy. J Cell Physiol 2018; 233: 8930-8939.
[27] Di Nardo A, Wertz MH, Kwiatkowski E, Tsai PT, Leech JD, Greene-Colozzi E, Goto J, Dilsiz P, Talos DM, Clish CB, Kwiatkowski DJ and Sahin M. Neuronal Tsc1/2 complex controls autophagy through AMPK-dependent regulation of ULK1. Hum Mol Genet 2014; 23: 3865-3874.
[28] Rosenfeldt MT, O'Prey J, Flossbach L, Nixon C, Morton JP, Sansom OJ and Ryan KM. PTEN deficiency permits the formation of pancreatic cancer in the absence of autophagy. Cell Death Differ 2017; 24: 1303-1304.
[29] Perl A. mTOR-dependent autophagy contributes to end-organ resistance and serves as target for treatment in autoimmune disease. Ebiomedicine 2018; 36: 12-13.
[30] Hu JG, Meng Y, Zhang ZQ, Yan QT, Jiang XW, Lv ZL and Hu LN. MARCH5 RNA promotes autophagy, migration, and invasion of ovarian cancer cells. Autophagy 2017; 13: 333-344.
[31] Zhu HT, Gan XL, Jiang XW, Diao S, Wu H and Hu JG. ALKBH5 inhibited autophagy of epithelial ovarian cancer through miR-7 and BCL-2. J Exp Clin Canc Res 2019; 38: 163.
[32] Boya P, Gonzalez-Polo RA, Casares N, Perfettini JL, Dessen P, Larochette N, Metivier D, Meley D, Souquere S, Yoshimori T, Pierron G, Codogno P and Kroemer G. Inhibition of macroautophagy triggers apoptosis. Mol Cell Biol 2005; 25: 1025-1040.
[33] Jin SK and White E. Role of autophagy in cancer - management of metabolic stress. Autophagy 2007; 3: 28-31.
[34] Ma L, Wang ZD, Xie MY, Quan YL, Zhu WY, Yang FM, Zhao CH, Fan Y, Fang N, Jiang HN, Wang Q, Wang SY, Zhou JW, Chen XF and Shu YQ. Silencing of circRACGAP1 sensitizes gastric cancer cells to apatinib via modulating autophagy by targeting miR-3657 and ATG7. Cell Death Dis 2020; 11: 169.
[35] Zhou FX, Yang XS, Zhao H, Liu Y, Feng Y, An R, Lv XH, Li J and Chen BL. Down-regulation of OGT promotes cisplatin resistance by inducing autophagy in ovarian cancer. Theranostics 2018; 8: 5200-5212.
[36] Wan BA, Dai LHY, Wang L, Zhang Y, Huang H, Qian GH and Yu TH. Knockdown of BRCA2 enhances cisplatin and cisplatin-induced autophagy in ovarian cancer cells. Endocr-Relat Cancer 2018; 25: 69-82.
[37] Gao N and Ye BG. Circ-SOX4 drives the tumorigenesis and development of lung adenocarcinoma via sponging miR-1270 and modulating PLAGL2 to activate WNT signaling pathway. Cancer Cell Int 2020; 20: 2.

[38] Lin WM, Ye HY, You KL and Chen L. Up-regulation of circ_LARP4 suppresses cell proliferation and migration in ovarian cancer by regulating miR-513b-5p/LARP4 axis. Cancer Cell Int 2020; 20: 5.
[39] Guan X, Zong ZH, Liu Y, Chen S, Wang LL and Zhao Y. circPUM1 promotes tumorigenesis and progression of ovarian cancer by sponging miR-615-5p and miR-6753-5p. Mol Ther-Nucl Acids 2019; 18: 882-892.
[40] Chaffer CL and Weinberg RA. A perspective on cancer cell metastasis. Science 2011; 331: 1559-1564.
[41] Liu Y, Li HY, Ban ZY, Nai MM, Yang L, Chen YN and Xu YM. Annexin A2 inhibition suppresses ovarian cancer progression via regulating beta-catenin/EMT. Oncol Rep 2017; 37: 3643-3650.
[42] Wu MH, Sun YQ, Xu FP, Liang YQ, Liu H and Yi YM. Annexin A2 Silencing Inhibits Proliferation and Epithelial-to-mesenchymal Transition through p53-dependent pathway in NSCLCs. J Cancer 2019; 10: 1077-1085.
[43] Bao J, Xu Y, Wang QY, Zhang JP, Li ZJ, Li DY and Li JS. miR-101 alleviates chemoresistance of gastric cancer cells by targeting ANXA2. Biomed Pharmacother 2017; 92: 1030-1037.